

# Age, growth and mortality of the goldlined seabream *Rhabdosargus sarba* in waters off southwestern Taiwan

By Shoou-Jeng Joung, Yu-Yung Shyh, Kwang-Ming Liu\*,  
and Shyh-Bin Wang

## Abstract

Age, growth and mortality of the goldlined seabream, *Rhabdosargus sarba*, were estimated based on 593 and 6516 specimens that were collected in waters off southwestern Taiwan from September 2015 to August 2016, and April 2015 to December 2017, respectively. The body weight (BW) and total length (TL) relationship (all data-pooled) was expressed as:  $BW = 0.01511 TL^{3.0346}$  ( $r^2 = 0.95$ ;  $n = 593$ ). Growth rings (identified as opaque and translucent zones) were counted on 447 sectioned sagittal otoliths using a microscope under transmitted light and were counted up to 8 (42.0 cm TL) for both sexes. Edge analysis indicated that growth rings in otoliths were deposited once per year, and the opaque zone was formed in December. The von Bertalanffy growth function (VBGF) best fit the observed length at age data for *R. sarba*. The growth parameters ( $\pm$  standard error) of VBGF for *R. sarba* (all data-pooled) were estimated as:  $L_\infty = 53.94 \pm 3.71$  cm TL,  $k = 0.217 \pm 0.033$  yr<sup>-1</sup>,  $t_0 = -0.182 \pm 0.167$  yr ( $n = 447$ ). Total mortality estimated from a length converted catch curve was 0.655 yr<sup>-1</sup>, age-specific natural mortality and fishing mortality were estimated as 0.789-0.293 yr<sup>-1</sup> and 0.109-0.365 yr<sup>-1</sup>, respectively. The exploitation rate was estimated to be 0.440.

\*Corresponding Author E-mail: [kmliu@mail.ntou.edu.tw](mailto:kmliu@mail.ntou.edu.tw)

This **early view** paper has been peer-reviewed and accepted for publication in *Pacific Science*. However, it has not been copy-edited nor has it undergone typesetting for *Pacific Science*. The final published paper will look different due to formatting changes, but scientific content will remain the same.

*Pacific Science*, vol. 73, no. 3  
May 17, 2019 (Early view)



Official Journal of the Pacific Science Association

## Introduction

The goldlined seabream *Rhabdosargus sarba* (Forsskål 1775) is widely distributed in the Indo-West Pacific: the Red Sea and East Africa to Japan, China, and Australian waters and it is a popular species for recreational and aquaculture fisheries in these regions (Smith and Heemstra 1986, Yeung and Chan 1987, Van der Elst 1988, El-Agamy 1989, Kailola et al. 1993, Leu 1994). This species can be found in the western, southern, and northern waters of Taiwan (Shao 2018). *Rhabdosargus sarba* inhabits rocky areas in coastal waters at the depths of 0-60 m and its major prey items are algae, mollusks, demersal invertebrates, and crustaceans (Blaber, 1984, Sommer et al. 1996, Rowling et al. 2010).

There are three categories of seabream in the Taiwanese catch statistics, namely the red seabream, *Pagrus major*, the black seabream, *Acanthopagrus schlegelii*, and other seabreams. Annual yields of other seabreams including *R. sarba* (the majority based on our fish market survey) in Penghu waters, southwestern Taiwan declined dramatically from 3825 tons in 2006 to 521 tons in 2016 (Taiwan Fisheries Statistic Year Book, Anon 2017). As no substantial reduction of fishing effort was noted, the decrease of catch implied that these stocks, mainly caught by pole and line, longline, and gill net as well as recreational fisheries in coastal waters off Penghu, may have experienced heavy exploitation over the past decade. A restocking program has been undertaken by releasing fry (8-10 cm TL) tagged with conventional tags (T-bar) in the southwestern waters of Taiwan in recent years to recover and enhance the stock size. Unfortunately, species-specific yield data for *R. sarba* are not available in the Taiwanese fisheries statistics.

*Rhabdosargus sarba* is a rudimentary hermaphrodite, with juveniles that develop into either males or females having ovarian and testicular zones of the gonads, respectively (Hesp and Potter 2003). Since exploitation is often size- and sex-selective, the impact of any fishing on a

sex-changing species will therefore depend on the type of hermaphroditism exhibited, their size-at maturity, and any size regulations for retention, like minimum legal length.

Age and growth of *R. sarba* has been described by several authors using ring counting in otoliths or length-frequency analysis in different waters (Radebe et al. 2002, Hughes et al. 2008, Grandcourt et al. 2011, Farrag et al. 2017). However, large inconsistencies among studies have been found. For example, the maximum observed length was 68.3 cm fork length (FL) in South Africa waters (Radebe et al. 2002), but it was 34.9 cm FL in Australia waters (Hughes et al. 2008), and 39 cm FL and 43.2 cm FL in Arabian waters (Farrag et al. 2017, Mehanna et al. 2012). Large discrepancies in growth parameters have also been noted. The estimated asymptotic length ( $L_{\infty}$ ) and growth coefficient ( $k$ ) of *R. sarba* were 71.5 cm FL and  $0.16 \text{ yr}^{-1}$  in South Africa (Radebe et al. 2002) but they were 26.4 cm FL and  $0.39 \text{ yr}^{-1}$  in the eastern Australia waters (Hughes et al. 2008) and 26.8 cm FL and  $0.59 \text{ yr}^{-1}$  in the western Australian waters (Hesp et al. 2004).

Biological information of *R. sarba* in Taiwan's waters is still limited and mainly on pathology and aquaculture. For example, studies have been done on the effect of tributyltin on reproduction and hatching (Dong 2005), molecular cloning and characterization (Chang 2006), and the effect of fishmeal on the growth of *R. sarba* (Wei 2011). However, age, growth and mortality information that is essential for stock assessment is still lacking for this species in Taiwan's waters. To fill this research gap, this study aims to provide the first information on age, growth and mortality of *R. sarba* in waters off southwestern Taiwan. In addition, growth parameters among different regions were compared.

## **MATERIALS AND METHODS**

### **Specimen collection**

Specimens caught by longline, pole and line, and gill net in the waters off southwestern Taiwan (Figure 1) were opportunistically collected monthly from April 2015 to December 2017 at the fish market in southwestern Taiwan. Measurements were made of total length (TL, in 0.1 cm) of these specimens. A subsample opportunistically collected from these specimens during September 2015 to August 2016 was brought back to our laboratory for further processing and age analysis. Body weight (BW, in 0.1 g) of these subsamples was measured and sex was identified by macroscopic examination of the gonads of each specimen.

To be able to estimate the weight (BW) of a sampled fish when only its TL was available, the relationship between  $BW$ - $TL$  was estimated using a nonlinear least squares regression model as:  $BW = a TL^b$ , where  $a$ ,  $b$  are parameters to be estimated. To facilitate the comparison with other studies where length measurement was not expressed in TL, the relation between TL and FL was expressed as:  $TL = a + bFL$ . An analysis of covariance (ANCOVA) was used to compare the TL-FL relationships between sexes.

### **Age determination**

Sagittal otoliths taken from each specimen of the subsample were rinsed in  $H_2O_2$  solution to remove connective tissue and then dried in an oven at 45°C for 24 hrs. Several techniques such as burning or glycerin dropping on the whole otolith, and sectioning along the long axis of the otolith were tried to increase the clarity of growth rings in otoliths in this study, but none of them improved the clarity of peripheral rings. Ultimately, sectioning along the short axis of otolith provided the best observations and had the highest success rate.

Otoliths were embedded in a mixture of Epoxy and Hardener with a ratio of 5:1. The embedded otoliths were then sectioned in a thickness of 0.05-0.2 mm along the short axis using an Isomet low-speed saw (Buehler, Lake Bluff, IL, USA). The sectioned otoliths were polished

with 800 and 1200-grain sand paper and fine polished using flannel with 0.05  $\mu\text{m}$   $\text{Al}_2\text{O}_3$ . Fine polished otoliths were examined under a stereo microscope (BX50F-3, Olympus, Tokyo, Japan) with transmitted light at 40 X magnification. The otolith images were captured by an attached digital camera (PowerShot D10, Canon, Tokyo, Japan).

Growth rings on the otolith images were counted without the knowledge of length and sex of specimens using the image process package (Adobe Photoshop CS4 11.0) to increase the brightness and contrast of the images to enhance the ring pattern (Figure 2). One growth ring includes one opaque and one translucent zone (Hughes et al. 2008). Opaque zones on otolith images were counted twice by the same reader. The time interval between the two readings was at least two weeks. If the two counts were different, then the otolith was recounted, and the final count was accepted if it agreed with one of the previous counts. If the third count did not match one of the previous two counts, the sample was discarded.

The index of average percentage error (IAPE) (Beamish and Fournier 1981) was used to estimate the reproducibility of the age estimation between two readings (Campana 2001). The equation used for IAPE is as:

$$\text{IAPE} = \frac{1}{N} \sum \square,$$

where  $N$  is the number of fish aged,  $R$  is the number of readings,  $X_{ij}$  is the count from the  $j$ th fish at the  $i$ th reading, and  $\bar{X}_j$  is the mean count of the  $j$ th fish from  $i$  readings.

The periodicity of ring formation was estimated from edge analysis (EA) and further verified by Okamura and Semba's (2009) approach that combines binary data with a statistical model for circular data with a sine pattern. A bias corrected Akaike information criterion ( $\text{AIC}_c$ , Hurvich and Tsai 1989) was used to select the most probable periodicity of ring formation (annual, biannual, and no cycle). As the spawning season of this species was from late November

to March (Lin et al. 1988, 1989), the birth date was assumed to be 1 February. The opaque zone was assumed to be formed in December annually (see Results) and the age (years) of each specimen was estimated using the following formulae by assuming the first ring was formed 10 months after birth:

$$\text{Age} = (m - 14) / 12 + n, \text{ if } m = 12,$$

$$\text{Age} = (m - 2) / 12 + n, \text{ if } m < 12,$$

where  $n$  is the number of rings, and  $m$  is the time (month) when the fish was captured.

### Growth functions

Three growth functions namely the von Bertalanffy (VBGF, Beverton 1954), the Robertson (Robertson 1923), and the Gompertz (Gompertz 1825) were used to fit the observed length-at-age. The three growth functions are described as follows:

2006. von Bertalanffy growth function (VBGF, Beverton 1954)

$$L_t = L_\infty (1 - e^{-k(t-t_0)}),$$

where  $L_t$  is the length-at-age  $t$ ,  $L_\infty$  is the asymptotic length,  $k$  is the growth coefficient,  $t$  is the age (years after birth), and  $t_0$  is the theoretical age at length 0.

(2) Robertson (Logistic) growth function (Robertson 1923, Ricker 1979)

,

where  $c_R$  and  $k_R$  are the parameter and the growth coefficient of the Robertson function, respectively.

(3) Gompertz growth function (Gompertz 1825)

,

where  $c_G$  and  $k_G$  are the parameter and growth coefficient of the Gompertz function.

The Gauss-Newton algorithm in the NLIN procedure of the statistical package SAS ver. 9.4 (SAS Institute 2014, Cary, NC, USA) was used in fitting the growth functions. The goodness of fit of the three growth functions was judged based on the bias corrected Akaike Information Criterion ( $AIC_c$ ) (Hurvich and Tsai 1989).  $AIC_c$  was expressed as:

$$AIC_c = AIC + \frac{2K(K+1)}{n-K-1},$$

where  $AIC = n \times \ln(\text{MSE}) + 2K$  (Akaike 1973),  $n$  is the total sample size, MSE is the mean square of the residuals, and  $K$  is the number of parameters estimated in the growth function. The  $AIC_c$  difference ( $\Delta AIC_c$ ) of each model was calculated as the difference of  $AIC_{c,i}$  and the lowest observed  $AIC_c$  value ( $AIC_{c,\min}$ ). Models with  $\Delta AIC_c$  values lower than 2 have good support, while those with values greater than 10 have no support (Burnham and Anderson 2002). A Chi-square test of maximum likelihood ratios (Kimura 1980) was used to examine the differences between sexes in the growth models.

In addition to the aforementioned data, 14 tagged artificially hatched fry were recaptured after being released for 9-467 days. These known length and age data were used to verify the estimated growth parameters.

Total mortality ( $Z$ ) was estimated based on Pauly's (1983) length-converted catch curve analysis:

$\ln[n(L_1-L_2)/dt] = a - Zt_{(L_1+L_2)/2}$ , where  $n(L_1-L_2)$  is catch in number between the length interval  $L_1$  and  $L_2$ ,  $dt$  is age difference between  $L_1$  and  $L_2$ ,  $a$  is a constant, and  $t$  is the age at the midpoint of  $L_1$  and  $L_2$ . Two methods were used to estimate natural mortality: age-specific natural mortality ( $M_t$ ) was estimated based on  $M_t = (1.92 \text{ yr}^{-1}) W_t^{-0.25}$  (Peterson and Wroblewski, 1984), where  $W_t$  is weight (in g) at age  $t$ ; a fixed  $M$  was estimated from Jensen's (1996) equation,  $M = 1.6 k$ ,

where  $k$  is the growth coefficient. Fishing mortality ( $F$ ) was then estimated as  $F = Z - M$ , and the exploitation rate ( $E$ ) was estimated as  $E = (F/Z)$  (King 2007).

## RESULTS

### Sample details

In total, TLs of 6516 specimens ranging from 8.0 to 49.0 cm TL were measured from April 2015 to December 2017. These data were used to estimate mortality. Among them, 593 specimens including 325 females, 225 males, 35 sex unidentified, and 8 hermaphrodite individuals were opportunistically collected as the subsample for age analysis (Table 1). Females ranged from 12.3 to 44.0 cm TL with the majority ranging from 22.0-32.0 cm TL and 25.4-1832.0 g BW. Males ranged from 14.6 to 44.0 cm TL with the majority ranging from 22.0-32.0 cm TL and 56.5-1600.0 g BW (Table 1). Sex unidentified fish ranged from 12.4 to 23.7 cm TL and 28.9-249.9 g BW; hermaphrodite individuals were in the range of 19.7-29.3 cm TL and 126.8-371.1 g BW (Table 1)(Figure 3).

### Fork length-total length relationship

The ANCOVA indicated that sex-specific FL-TL relation was not significantly different ( $P > 0.05$ ) and the FL-TL relation (sexes combined) was expressed as:

$$FL = 0.022 + 0.9228TL \quad (r^2 = 0.993, n = 458, P < 0.05).$$

### BW-TL relationship

The maximum likelihood ratio test showed no significant difference in BW-TL relationships between sexes. Thus, the BW-TL relationship for all data-pooled (males, females, sex unidentified, and sex reversing) was estimated as:

$$BW = 0.01511TL^{3.0346} \quad (r^2 = 0.950, n = 593, \text{Figure 4}).$$

### Age estimate and precision



In total, 146 otoliths were discarded due to failure in processing or inconsistency in the three ring counts ( $n = 16$ ) and consequently 447 otoliths (264 females, 149 males, 26 sex unidentified, and 8 hermaphrodite) were used for age estimation and growth curve fitting. The maximum number of growth rings counted was 8 (42.0 cm TL) for both sexes (Table 2). The IAPE was 4.85% which was less than Campana's (2001) criterion of 5.5% and the age-bias plot of the two readings is showed in Figure 5.

### **Periodicity of ring formation**

The edge analysis showed that the percentage of otoliths with an opaque edge increased gradually from the lowest value in May (5.26%) and peaked in December (66.67%) indicating that the growth ring was formed annually (Figure 6). The statistical analysis of Okamura and Semba (2009) also indicated that the one ring per year model had the highest support with the smallest  $AIC_c$  (574.0) compared with the no-cycle (602.2) and biannual cycle models (602.6). The results of the above edge analysis and the statistical method (Okamura and Semba 2009) provided some evidence that opaque zone was formed in December, and the periodicity of ring formation was one year.

### **Growth functions**

The estimated parameters and the  $AIC_c$ ,  $\Delta AIC_c$ , and  $w_i$  for each growth function by sex and for all data-pooled are showed in Table 3. The maximum likelihood ratio test indicated no significant difference in growth functions between sexes. Thus, all the three growth functions were expressed based on all data-pooled. The smallest  $AIC_c$  (938.4) and the highest  $w_i$  (0.507) of VBGF indicated that it is the best model for fitting the observed length-at-age data for *R. sarba*. However, the  $\Delta AIC_c$  value of the Gompertz function was less than 2 indicating that this growth function also has good support. The growth parameters ( $\pm$  standard error) of VBGF for *R. sarba*

(all data-pooled) were estimated as:  $L_{\infty} = 53.94 \pm 3.71$  cm TL,  $k = 0.217 \pm 0.033$  yr<sup>-1</sup>,  $t_0 = -0.182 \pm 0.167$  yr ( $n = 447$ ,  $P < 0.05$ ) (Figure 7).

Total mortality estimated from length-converted catch curve was 0.655 yr<sup>-1</sup>, age-specific natural mortality based on Petersen and Wroblewski (1984) and fishing mortality were estimated as 0.293 - 0.789 yr<sup>-1</sup> and 0.1094 - 0.3651 yr<sup>-1</sup>, respectively (Table 4). The fixed  $M$  estimated based on Jensen's (1996) equation was 0.347 yr<sup>-1</sup> and  $F$  was 0.308 yr<sup>-1</sup>. Exploitation rate was estimated to be 0.44 and 0.47 for age-specific and fixed natural mortality, respectively.

## DISCUSSION

The present study provides an important contribution on the age and growth of *R. sarba* in the waters off southwestern Taiwan, which can be used as biological input parameters for a future stock assessment.

In this study, the specimens collected for age estimation were assumed to be from the wild because no tags were found on these fish although no confirmation was made by using molecular techniques. Among them, no specimens < 12.0 cm TL were collected and the maximum observed length (44.0 cm TL) is much smaller than the record of 80 cm TL in Southern Africa waters (Torres 1991) suggested that the growth parameters derived in this study may not appropriate to describe the whole life history of *R. Sarba* if similar maximum size fish exists in Taiwanese waters. Also, it is possible that such large-sized fish do not occur in Taiwanese waters. The discrepancy in maximum size between *R. sarba* from southern Africa and everywhere else has been suggested to be a result of *R. sarba* in southern Africa not being the same species as occurs elsewhere. The lack of small and large specimens may be due to the following reasons: (1) gear selectivity prevented catching very small and very large fish, (2) the nursery ground of this species was not covered by the fishing activities. *Rhabdosargus sarba*

shifted its habitat with age in western Australian waters i.e., juveniles were found in the coastal waters and adults were in offshore and deeper waters (Hesp et al. 2004). Therefore, to collect very small-sized fish, a nearshore fishery-independent survey using smaller mesh size is needed in the future. To collect very large-size fish, an offshore longline vessel operating in deep waters is suggested.

*Rhabdosargus sarba* is a rudimentary hermaphrodite with gonads becoming testis earlier than ovary (Garratt 1993). This might explain why the sex of some specimens could not be identified and some were found with testis and ovary simultaneously. As no significant differences on the relationships of BW-TL, FL-TL, and growth between sexes were found, these relationships were described based on all data-pooled. Thus, the rudimentary hermaphroditism does not likely affect the results derived in the present study.

Several explanations for growth ring formation have been proposed such as temperature, feeding, physical condition and spawning (Yin 1998). When a fish reaches maturity, energy may be allocated to reproduction in spawning season that could result in ring formation due to reduced growth. Steward et al. (2009) mentioned that ring formation in the otoliths of gray angelfish (*Pomacanthus arcuatus*) occurs during the spawning season. Shimose and Tachihara (2005) and Akihiko et al. (2010) also concluded that ring formation in otoliths is related to the spawning behavior of the blackspot snapper *Lutjanus fulviflammus* and the blackspot tuskfish *Choerodon schoenleinii* in the waters off Okinawa Island, Japan. For *R. sarba*, the spawning season occurs mainly from the end of winter to the spring but varies in different waters. Wallace (1975) documented that the spawning season of this species is from July to November and it overlaps with the timing of ring formation (September to December) in South Africa waters (Radebe et al. 2002). The spawning season is from November to March but the ring formation occurs after spawning (May-August) for *R. sarba* in southern Gulf of Arabian (Grandcourt et al.

2011). In this study, the timing of ring formation (December to February) corresponds with the spawning season (late November to March, Lin et al. 1989) suggesting ring formation in otoliths may be closely related to spawning. The lowest sea surface temperature (SST) in waters off southwestern Taiwan occurs in January and February (1998-2016) (Anon 2016), corresponding to the time of ring formation suggesting that ring formation is also likely related to the low SST.

The marginal increment ratio (MIR) and EA are two methods commonly used for verifying the periodicity of ring formation. Although only EA was applied in this study, the result of one ring per year was further supported by cycle analysis (Okamura and Semba 2009). Similar conclusions have been made by several authors for *R. sarba* in eastern Australian waters, South Africa, and Oman waters in the Gulf of Arabia, respectively (Hughes et al. 2008, Radebe et al. 2002, Grandcourt et al. 2011, Mehanna et al. 2012) suggesting verification of annual ring formation found in this study is robust.

The VBGF was chosen as the best growth function for *R. sarba* because of the smallest  $AIC_c$  and the largest  $w_i$ . However,  $\Delta AIC_c < 2$  for the Gompertz function suggests that it is also a good growth function for this species. The  $L_\infty$  derived from the VBGF (53.94 cm TL) and Gompertz function (47.80 cm TL) are greater than the maximum observed length of 44.0 cm TL suggesting both estimates are acceptable. The sizes at birth ( $L_0$ ) and at 0.5 year old ( $L_{0.5}$ ) were predicted to be 2.09 cm and 7.40 cm TL by the VBGF, and were 7.50 and 11.89 cm TL predicted by the Gompertz function. The  $L_0$  predicted by the VBGF seems more reasonable but it is likely overestimated by the Gompertz function because the mean observed length of  $L_{0.5}$  was 9.57 cm TL based on the measurements of 60 artificially hatched fry before releasing. As aquaculture ponds may have more food, better water quality and food quality than those in the wild, the actual value of  $L_{0.5}$  for the wild *R. sarba* should be smaller than 9.57 cm TL. Because the VBGF

has better predictions for the  $L_0$  and  $L_{0.5}$ , VBGF was chosen to be the best growth function for *R. sarba*.

The estimated  $k$  for *R. sarba* in this study was comparable with that in the Arabian Gulf (Farrag et al. 2017), but was greater than that in the South Africa (Radebe et al. 2002) and was smaller than those in eastern Australia waters (Hughes et al. 2008), the Arabian Sea (Mehanna et al. 2012), and the southern Arabian Gulf (Grandcourt et al. 2011) (Table 4). The estimated  $L_\infty$  in the present study is comparable with those in the Arabian Sea (Mehanna et al. 2012) and in the Arabian Gulf (Farrag et al. 2017) but is quite different from those in South Africa (Radebe et al. 2002), in the southern Arabian Gulf (Grandcourt et al. 2011), and in western and eastern Australian waters (Hesp et al. 2004, Hughes et al. 2008) (Table 5).

The lengths of tag and recaptured individuals are larger than those predicted by VBGF before age 2 (Figure 8). The TLs of two individuals released for 467 days correspond with the predicted values from the VBGF. These findings suggested that the fry from aquaculture may grow faster than those from the wild for a certain time period after release and reach similar size when they approach age 2.

The growth curve derived from this study is comparable with those from the Arabian Gulf (Farrag et al. 2017) but is different from those from other regions (Figure 9). The large discrepancy of growth curves in different studies may be due to (1) different size composition of specimens used in aging analysis among studies, (2) geographic differences, and (3) different stocks. As the specimens used in this study were mainly from ages 2 and 3 (22.0-32.0 cm TL, 77.6%), sampling bias is likely to be an important factor affecting the estimates of growth parameters in addition to geographic differences. Hesp et al. (2004) mentioned that size composition of samples collected in different habitats (coastal, nearshore, or offshore) may result in a discrepancy in growth estimation. In addition, species misidentification cannot be ruled out

because such a large discrepancy in growth parameters does not likely occur for a same species in different regions. Kuitert (1993) suspected that there may be more than one species being reported as *R. sarba*, however further study is needed to clarify this .

The exploitation rate of this stock, either derived from age-specific or the fixed  $M$ , is approaching to the optimum exploitation rate (0.5) (King 2007) suggesting that this stock is in optimum exploitation. To ensure sustainable utilization of this stock, continuous monitoring of catch and size composition is suggested.

In conclusion, this study provides the first detailed estimates of the age and growth for *R. sarba* in waters off southwestern Taiwan that can be used for future stock assessment. However, the growth parameters obtained in this study can be improved by collecting more specimens of very small and very large fish. The possible reasons for large discrepancies in growth parameters among worldwide locations where the species is found also needs further study.

### **ACKNOWLEDGEMENTS**

Financial support for this study was provided by the Fisheries Agency, Council of Agriculture, Taiwan, R.O.C., Grants FA105-AS-14.2.3-F-F3 and FA106-AS-14.2.3-F-F3.

### **Literature Cited**

Akaike, H. 1973. Information theory and an extension of the maximum likelihood principle.

Pages 267-281 in B. N. Peetov and F. Csaki, eds. Second international symposium on information theory. Budapest: Akademiai kiado, Hungary.

Akihiko, E., K. Kiyooki, and K. Toshihiko. 2010. Growth, sex ratio, and maturation rate with age in the blackspot tuskfish *Choerodon schoenleinii* in waters off Okinawa Island, southwestern Japan. Fish. Sci. 76: 577-583. doi: 10.1007/s12562-010-0244-4.

- Anon. 2016. Central Weather Bureau, Taiwan. [https://www.cwb.gov.tw/V7/climate/marine\\_stat/wtmp.htm](https://www.cwb.gov.tw/V7/climate/marine_stat/wtmp.htm). Accessed 21 March 2018.
- Anon. 2017. Taiwan Fisheries Statistic Year Book, Fisheries Agency, Council of Agriculture, Taiwan. <https://www.fa.gov.tw/cht/PublicationsFishYear/>. Accessed 21 March 2018.
- Beamish, R. J., and D. A. Fournier 1981. A method for comparing the precision of a set of age determinations. *Can. J. Fish. Aquat. Sci.* 38: 982-983. doi: 10.1139/f81-132.
- Beverton, R. J. H. 1954. Notes on the use of theoretical models in the study of the dynamics of exploited fish populations. Miscellaneous Contribution 2. Beaufort, NC: US Fisheries Laboratory. 159 pp.
- Blaber, S. J. M. 1984. The diet, food selectivity and niche of *Rhabdosargus sarba* (Teleostei: Sparidae) in Natal estuaries. *South Afr. J. Zool.* 19: 241-246. doi: 10.1080/02541858.1984.11447885
- Burnham, K. P., and D. R. Anderson. 2002. Model Selection and multimodel inference: A practical-theoretic approach. New York: Springer, 488 pages.
- Campana, S. E. 2001. Accuracy, precision and quality control in age determination, including a review of the use and abuse of age validation methods. *J. Fish. Biol.* 59: 197-142. doi: 10.1111/j.1095-8649.2001.tb00127.x.
- Chang, C. F. 2006. Molecular cloning and characterization of cyp 19 genes of silver sea bream (*Rhabdosargus sarba*) and the impacts of cyp19 genes on the infertility of zebrafish (*Danio rerio*) and tilapia (*Oreochromis mossambicus*). Master thesis. National Taiwan Ocean University, Keelung, Taiwan, 100 pp. (In Chinese)
- Dong, R. P. 2005. The effects of tributyltin (TBT) on reproduction and hatching of yellow sea bream (*Rhabdosargus sarba*) in spawning season. Master thesis. National Taiwan Ocean University, Keelung, Taiwan, 71 pp. (In Chinese)

- El-Agamy, A. E. 1989. Biology of *Sparus sarba* (Forsskål) from the Qatari water, Arabian Gulf. J. Mar. Biol. Assoc. India. 31(1/2): 129-137.
- Farrag, E., A. Alzaby, and C. Subbiah. 2017. Some biological aspects and stock status of goldlined seabream *Rhabdosargus sarba* (Forsskål, 1775) from the Arabian Gulf of the United Arab Emirates. Comput. Biol. Bioinform. 5(4): 43-49. doi: 10.11648/j.cbb.20170504.11.
- Garratt, P. A. 1993. Comparative aspects of the reproductive biology of seabreams (Pisces: Sparidae) [dissertation]. Rhodes University, Grahamstown, South Africa. 175 pp.
- Gompertz, B. 1825. On the nature of function expressive of the law of human mortality and on a new mode of determining life contingencies. Philos. Trans. Roy. Soc. London. Ser. A. 155: 513-585.
- Grandcourt, E, T. Z. Al Abdessalaam, F. Francis, and A. Al Shamsi. 2011. Demographic parameters and status assessments of *Lutjanus ehrenbergii*, *Lethrinus lentjan*, *Plectorhinchus sordidus* and *Rhabdosargus sarba* in the southern Arabian Gulf. J. Appl. Ichthy. 27: 1203-1211. doi: 10.1111/j.1439-0426.2011.01776.x.
- Hesp, S. A., and I. C. Potter. 2003. Reproductive biology of *Rhabdosargus sarba* (Sparidae) in Western Australian waters in which it is a rudimentary hermaphrodite. J. Mar. Biol. Assoc. U. K. 83: 1333-1346. doi: 10.1017/S0025315403008786.
- Hesp, L. M., N. G. Hall, and I. C. Potter. 2004. Size-related movements of *Rhabdosargus sarba* in three different environments and their influence on estimates of von Bertalanffy growth parameters. Mar. Biol. 114: 449-462. doi: 10.1007/s00227-003-1217-2.
- Hughes, J. M., J. Stewart, and B. W. Kendall. 2008. Growth and reproductive biology of tarwhine *Rhabdosargus sarba* (Sparidae) in eastern Australia. Mar. Freshw. Res. 59: 1111-1123. doi: 10.1071/MF08102.



- Hurvich, C. M., and C. L. Tsai. 1989. Regression and time series model selection in small samples. *Biomet.* 76: 297-307.
- Jensen, A. L. 1996. Beverton and Holt life history invariants result from optimal trade-off of reproduction and survival. *Can. J. Fish. Aquat. Sci.* 53: 820-822.
- Kailola, P. J., J. W. Meryl, P. Stewart, R. Reichelt, A. McNee, and G. Chris. 1993. Australian fisheries resources. Bureau of Resource Sciences, Department of Primary Industries and Energy, Fisheries Research and Development Corporation Canberra, Australian, 422 pp.
- King, M. 2007. *Fisheries Biology, Assessment and Management*, 2nd Edition. Wiley-Blackwell, 400 pp.
- Kimura, M. 1980. A simple method for estimating evolutionary rates of base substitutions through comparative studies of nucleotide sequences. *J. Molec. Evol.* 16: 111-120. doi: 10.1007/BF01731581.
- Kuiter, R. H. 1993. *The complete diver's and fishermen's guide to coastal fishes of South-Eastern Australia*. Bathurst, Australia: Crawford House Press.
- Leu, M. Y. 1994. Natural spawning and larval rearing of silver bream, *Rhabdosargus sarba* (Forsskål), in captivity. *Aquacul.* 120: 115-122. doi: 10.1016/0044-8486(94)90227-5.
- Lin, K. J., R. M. Chang, C. Y. Liu, Y. K. Fang, C. L. Chen, C. Y. Juang, and J. Y. Twu. 1988. Natural spawning of goldlined seabream *Sparus sarba* in the artificial environment and embryonic development. *Bull. Taiwan Fish. Res. Inst.* 45: 1-16. (In Chinese)
- Lin, K. J., R. M. Chang, J. Y. Twu, and C. Y. Liu. 1989. Experiments on the propagation of goldlined seabream *Sparus sarba* -- breeder culture, natural spawning in the artificial environment of 3-year-old breeder, and hatching of fertilized eggs. *Bull. Taiwan Fish. Res. Inst.* 47: 21-38. (In Chinese)

- Mehanna, S. F., F. R. Al-Kiyumi, and L. Al-Kharusi. 2012. Population dynamics and management of goldlined seabream *Rhabdosargus sarba* (Sparidae) from the Oman coast of Arabian Sea. *Fish. Aquacul. J.* 2012: FAJ-40.
- Okamura, H., and Y. Semba. 2009. A novel statistical method for validating the periodicity of vertebral growth band formation in elasmobranch fishes. *Can. J. Fish. Aquat. Sci.* 66(5): 771-780. doi: 10.1139/F09-039.
- Pauly, D. 1983. Some simple methods for assessment of tropical fish stocks. *FAO Fish. Tech. Pap.* 234: 52
- Petersen, I., and J. S. Wroblewski. 1984. Mortality rate of fishes in the pelagic ecosystem. *Can. J. Fish. Aquat. Sci.* 41: 1117-1120.
- Radebe, P. V., B. Q. Mann, L. E. Beckley, and A. Govender. 2002. Age and growth of *Rhabdosargus sarba* (Pisces: Sparidae), from KwaZulu-Natal, South Africa. *Fish. Res.* 58: 193-201. doi: 10.1016/S0165-7836(01)00383-6.
- Ricker, W. E. 1979. Growth rate and models. In: Hoar, W. S., D. J. Randall, and J. R. Brett. Eds., *Fish Physiology VIII, Bioenergetics and Growth*, Academic Press, New York, p 677-743.
- Robertson, T. B. 1923. *The chemical basis of growth and senescence*. Lippincott, New York, USA. 98 pp.
- Rowling, K., A. Hegarty, and M. Ives. 2010. Status of fisheries resources in NSW 2008/09. NSW Department of Primary Industries, Cronulla, Australia, p 337-339.
- Shao, K. T. 2018. Taiwan fish database. WWW Web electronic publication. <http://fishdb.sinica.edu.tw>. Accessed 21 March 2018.
- Shimose, T., and K. Tachihara. 2005. Age, growth and maturation of the blackspot snapper *Lutjanus fulviflammus* around Okinawa Island, Japan. *Fish. Sci.* 71: 48-55. doi:10.1111/j.1444-2906.2005.00929.x.

- Smith, M. M., and P. C. Heemstra. 1986. *Smith's Sea Fishes*. Springer-Verlag Berlin Heidelberg, New York, USA, 1047 pp.
- Sommer, C., W. Schneider, and J. M. Poutiers. 1996. *The living marine resources of Somalia (FAO species identification field guide for fishery purposes)*. Food and Agriculture Organization of the United Nations, Rome, Italy, 376 pp.
- Steward, C. A., K. D. Demaria, and J. M. Shenker. 2009. Using otolith morphometrics to quickly and inexpensively predict age in the gray angelfish (*Pomacanthus arcuatus*). *Fish. Res.* 99: 123-129. doi: 10.1016/j.fishres.2009.05.011.
- Torres, F. Jr. 1991. Tabular data on marine fishes from Southern Africa, part I. Length-weight relationship. *Fishbyte*. 9(1): 50-53.
- Van der Elst, R. P. 1988. *A guide to the common sea fishes of southern Africa*. Struik Publishers, Cape Town, Southern Africa, 398 pages.
- Wallace, J. H. 1975. The estuarine fishes of the east coast of South Africa: III. Reproduction. *Oceanogr. Res. Inst. Invest. Rep.* 41: 1-51.
- Wei, S. H. 2011. Effects of low fishmeal and non-fishmeal diets on the growth performance of silver sea bream (*Rhabdosargus sarba*). Master thesis. National Taiwan University, Taipei, Taiwan, 63 pages. (In Chinese)
- Yeung, W. S. B, S. T. H. Chan. 1987. The gonadal anatomy and sexual pattern of the protandrous, sex reversing fish. *Zool.* 212(3): 521-532. doi: 10.1111/j.1469-7998.1987.tb02922.x.
- Yin, M. C. 1998. *Fish Ecology*. The Sueichan Press. Keelung, Taiwan. 536 pp. (In Chinese)

TABLE 1. Details of *R. sarba* specimens collected in the present study.

Month/year	Female		Male		Sex unidentified	Hermaphrodit hermaphrodite		Total	
	n	TL (cm)	n	TL (cm)	n	TL (cm)	n	TL (cm)	n
Sep.-15	28	17.5-31.0	9	17.5-26.5	3	16.0-19.0			40
Oct.-15	30	15.3-34.0	13	15.9-31.4	6	14.8-18.0			49
Nov.-15	29	19.5-44.0	37	19.5-43.5	3	12.5-22.0			69
Dec.-15	19	12.3-43.0	10	27.0-38.0	0				29
Jan.-16	14	26.0-42.0	10	21.0-44.0	6	21.5-23.5	3	21.0-24.0	33
Feb.-16	12	18.5-42.0	17	19.5-42.0	1	18.5-18.5	2	23.5-25.5	32
Mar.-16	38	25.4-38.1	35	22.2-40.7	1	23.7-23.7	2	28.4-29.3	76
Apr.-16	38	20.5-42.0	18	21.0-40.0	2	21.0-21.0			58
May-16	9	17.9-20.2	8	18.7-21.7	3	18.8-20.1	1	19.7-19.7	21
Jun.-16	55	21.5-32.5	36	22.0-37.0	1	23.0-23.0			92
Jul.-16	22	14.4-36.5	15	14.6-39.0	9	12.4-16.3			46
Aug.-16	31	25.0-32.6	17	26.0-32.4	0				48
Total	325	12.3-44.0	225	14.6-44.0	35	12.4-23.7	8	19.7-29.3	593

TABLE 2. Age-length key of *R. sarba*.

TL (cm)	Age (year)								n
	1+	2+	3+	4+	5+	6+	7+	8+	
12-14	3								3
14-16	6								6
16-18	8								8
18-20	4	25							29
20-22	2	30							32
22-24	6	60	8						74
24-26	1	17	15						33
26-28	2	15	39						56
28-30		7	55	6					68
30-32		4	42	13					59
32-34		3	12	10					25
34-36		4	7	5					16
36-38			2	3	2				7
38-40			2	4	10				16
40-42					4	2			6
42-44					3	3	1	2	9
Total	32	165	182	41	19	5	1	2	447

TABLE 3. Comparison of goodness-of-fit among the three growth functions used to fit the observed length-at-age for *R. sarba* (all data-pooled, n=447).

Growth function	Parameters					
	$L_\infty$	$k/k_R/k_G$	$t_0/c_R/c_G$	$AIC_c$	$\Delta AIC_c$	$w_i$
von Bertalanffy	53.94	0.217	-0.182	938.40	0.00	0.507
Robertson (1923)	45.12	0.559	2.338	941.11	2.71	0.13
Gompertz (1825)	47.80	0.387	1.593	939.07	0.67	0.36

TABLE 4. Estimated natural mortality ( $M$ ), fishing mortality ( $F$ ) and total mortality ( $Z$ ) for goldlined seabream.

Age	$M$	$F$	$Z$
1+	0.789	0.0000	0.789
2+	0.545	0.109	0.655
3+	0.446	0.209	0.655
4+	0.392	0.263	0.655
5+	0.358	0.297	0.655
6+	0.336	0.319	0.655
7+	0.320	0.335	0.655
8+	0.308	0.347	0.655
9+	0.300	0.355	0.655
10+	0.293	0.362	0.655

TABLE 5. Comparison of growth parameters of *R. sarba* derived from different studies.

Region	$L_{\infty}$ (FL)	$k$	$t_0$	n	$t_{\max}$	Reference
Arabian Gulf	41.9	0.25	-0.58	5,085	8	Farrag <i>et al.</i> (2017)
Southern Arabian Gulf	25.3	1.29	-0.03	700	5	Grandcourt <i>et al.</i> (2011)
Eastern Australia	26.4	0.39	-0.56	739	16.5	Hughes <i>et al.</i> (2008)
Arabian Sea	41.5*	0.33	-0.83	1,185	6	Mehanna <i>et al.</i> (2012)
South Africa	71.5	0.16	-0.996	216	16	Radebe <i>et al.</i> (2002)
Southwestern Taiwan	49.8**	0.22	-0.182	447	8.2	Present study

\*: TL was converted to FL using Mehanna *et al.* (2012).

\*\* : TL was converted to FL using FL-TL relation derived from this study.

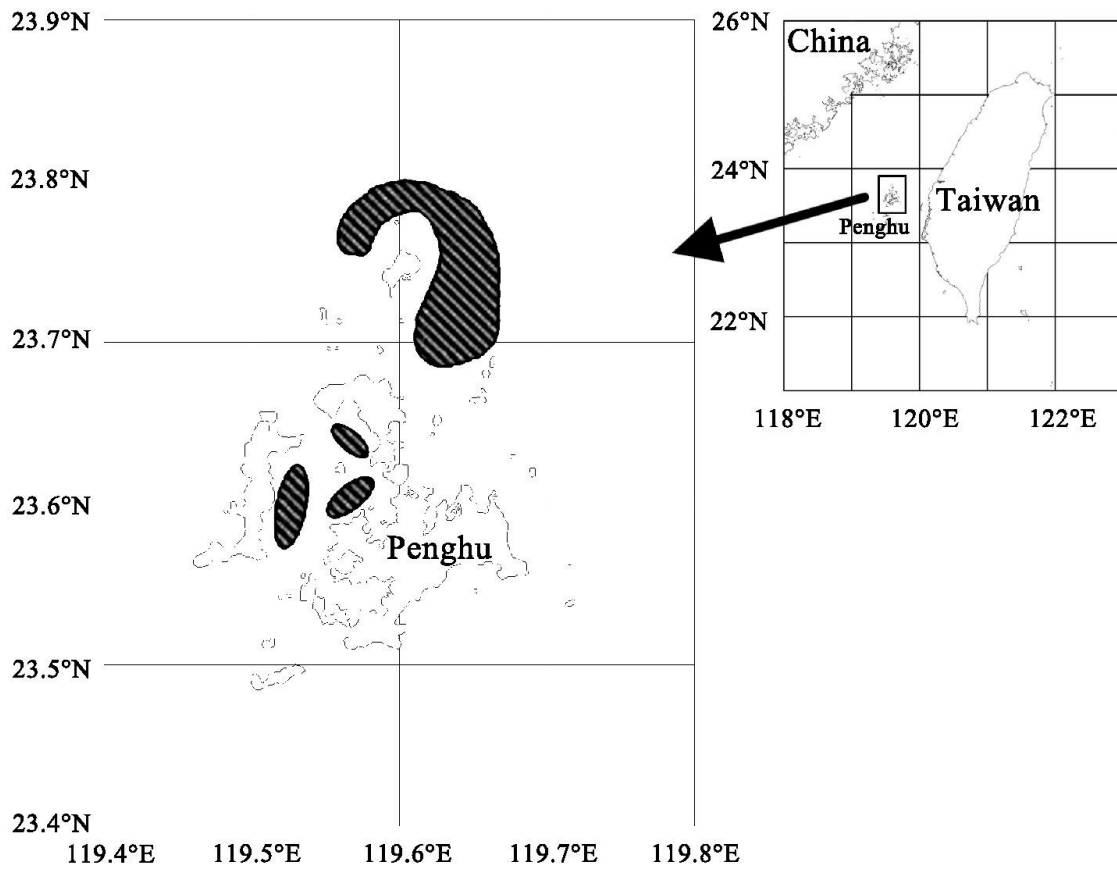


FIGURE 1. Sampling area of *R. sarba* in this study.



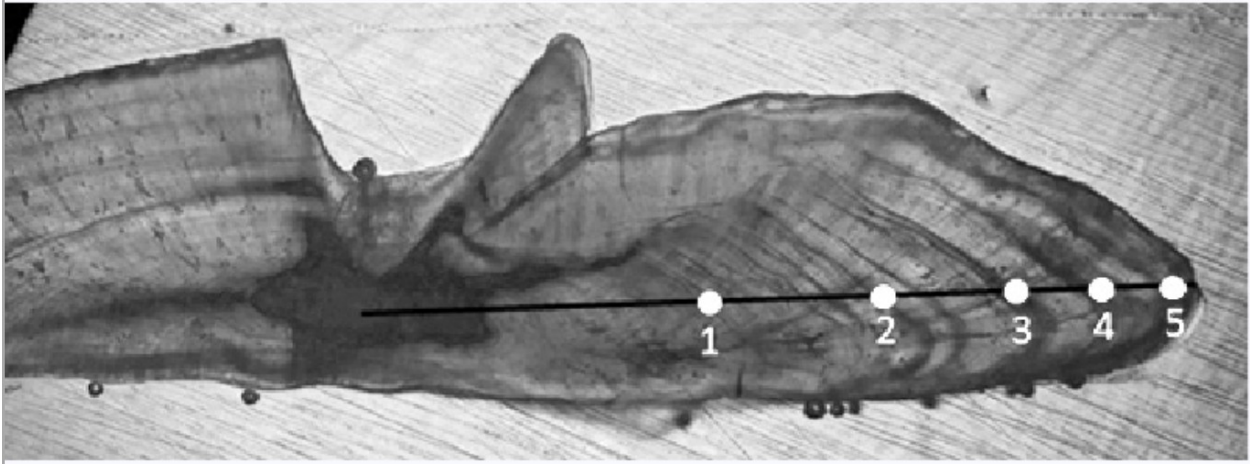


FIGURE 2. Image of sectioned otolith of *R. sarba* (from a 38.0 cm TL male) magnified by Adobe Photoshop CS4 11.0 and displayed on screen. The numbers indicate growth rings.

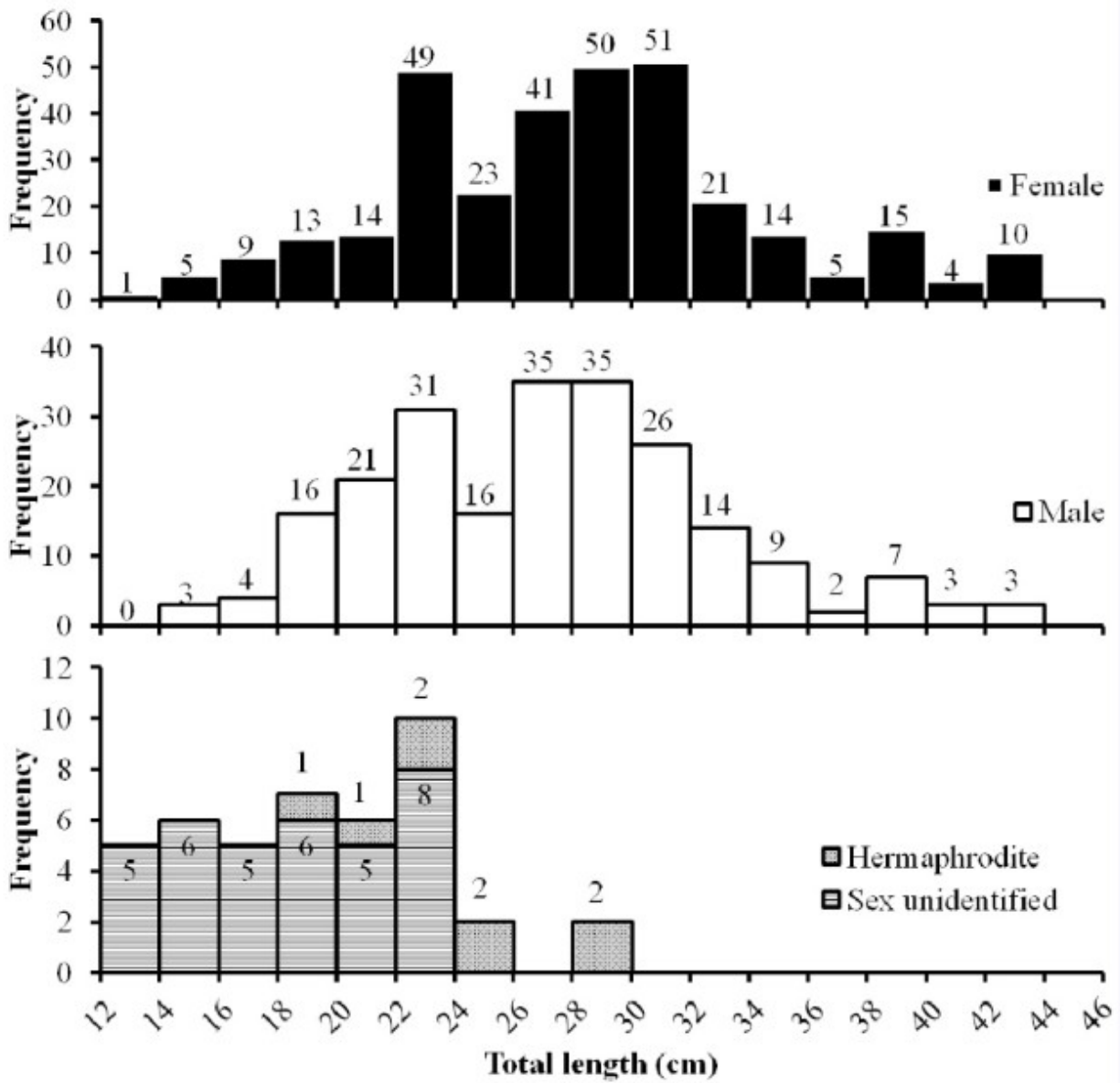


FIGURE 3. Total length frequency distribution of *R. sarba* in this study.

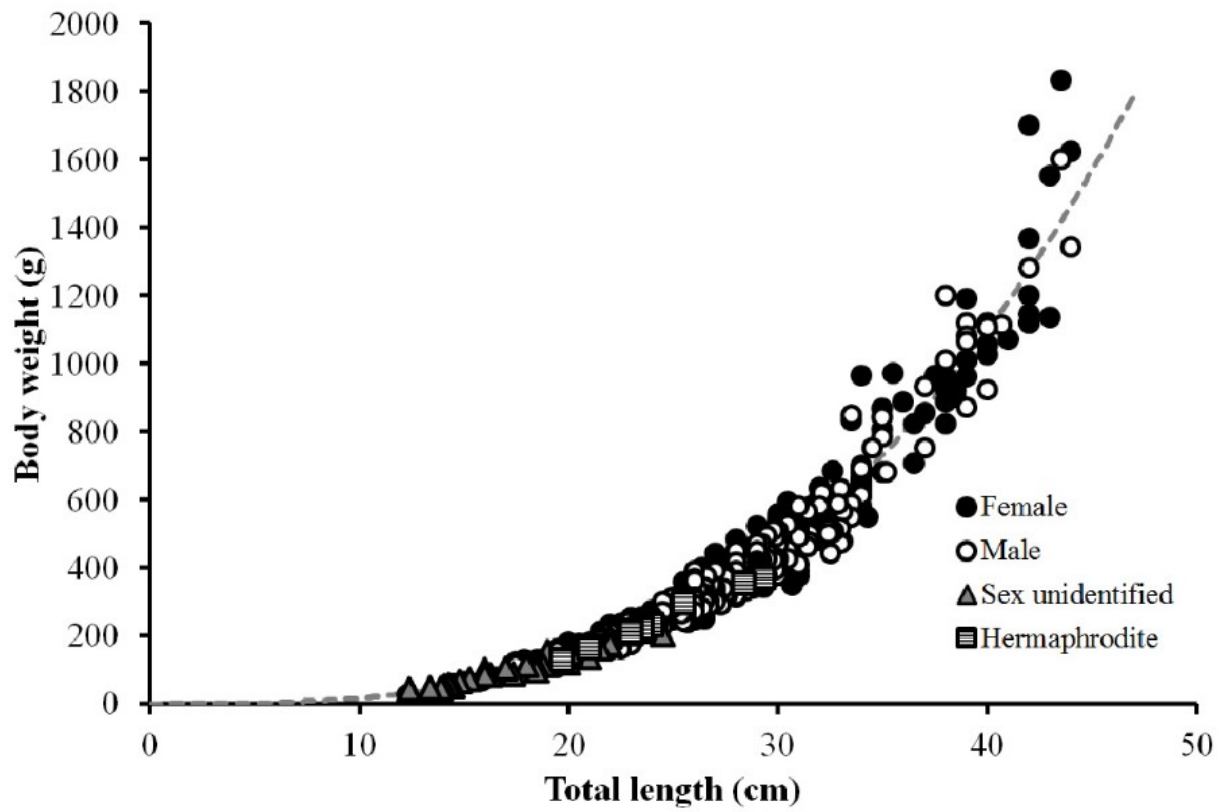


FIGURE 4. Relationship between total length (TL) and body weight (BW) of *R. sarba*.

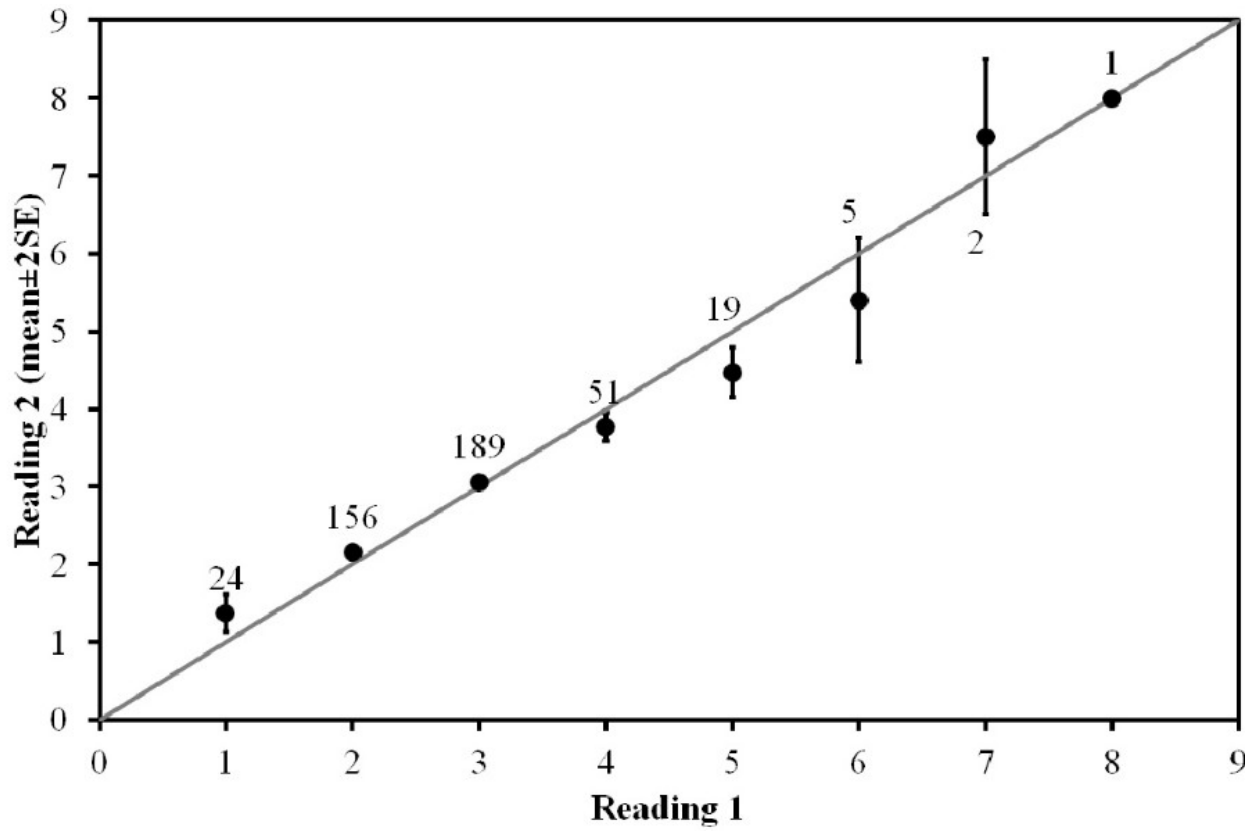


FIGURE 5. Age-bias plot for the comparison of otolith ring counts between reading 1 and reading 2 ( $\pm 2$  SE).

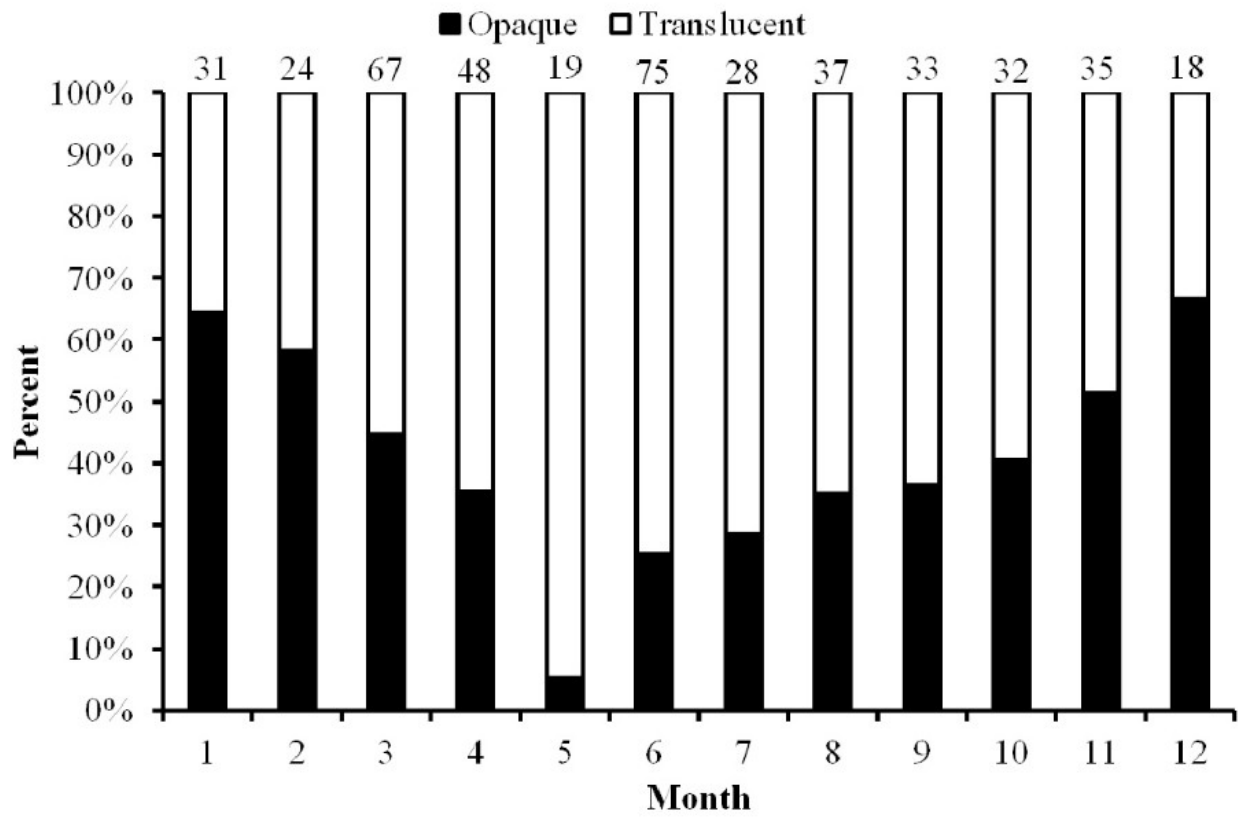


FIGURE 6. Edge analysis of growth ring formation of *R. sarba*.

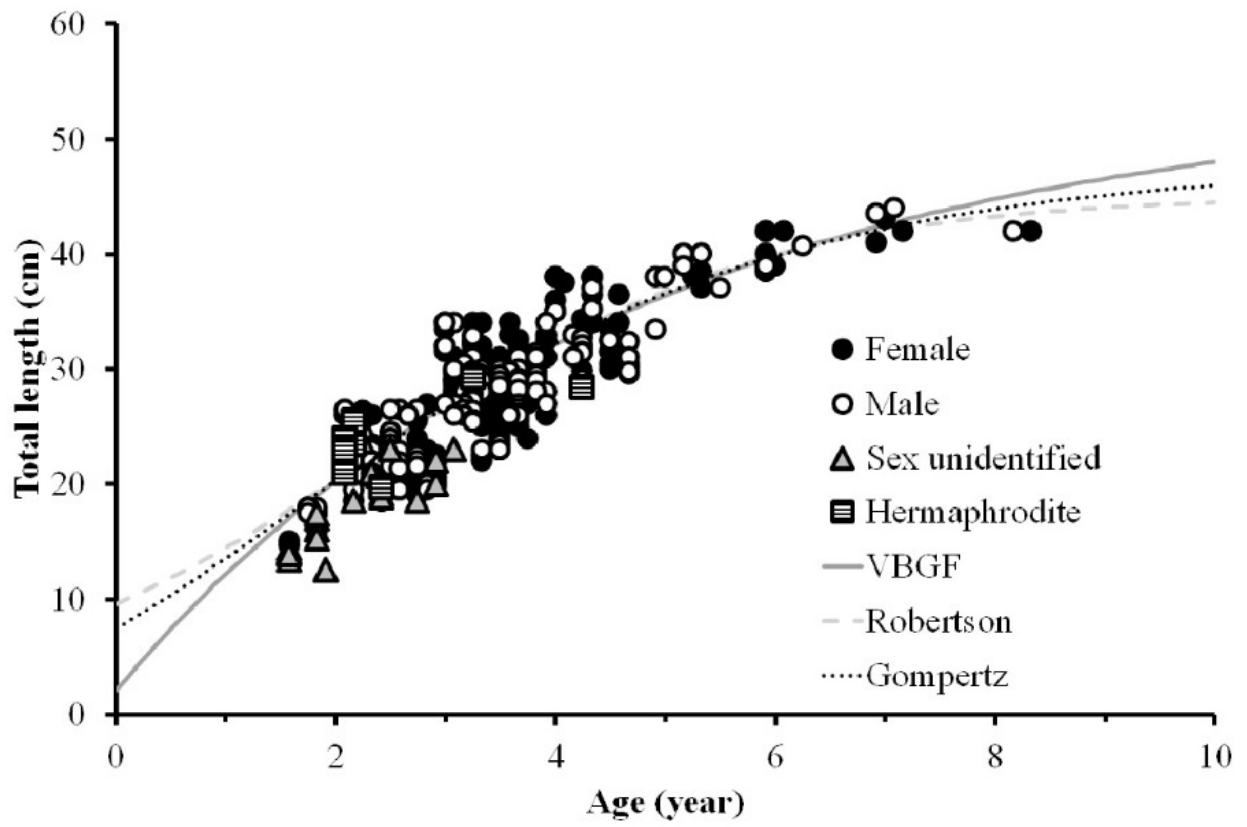


FIGURE 7. The three growth functions fit the observed length at age data of *R. sarba*.

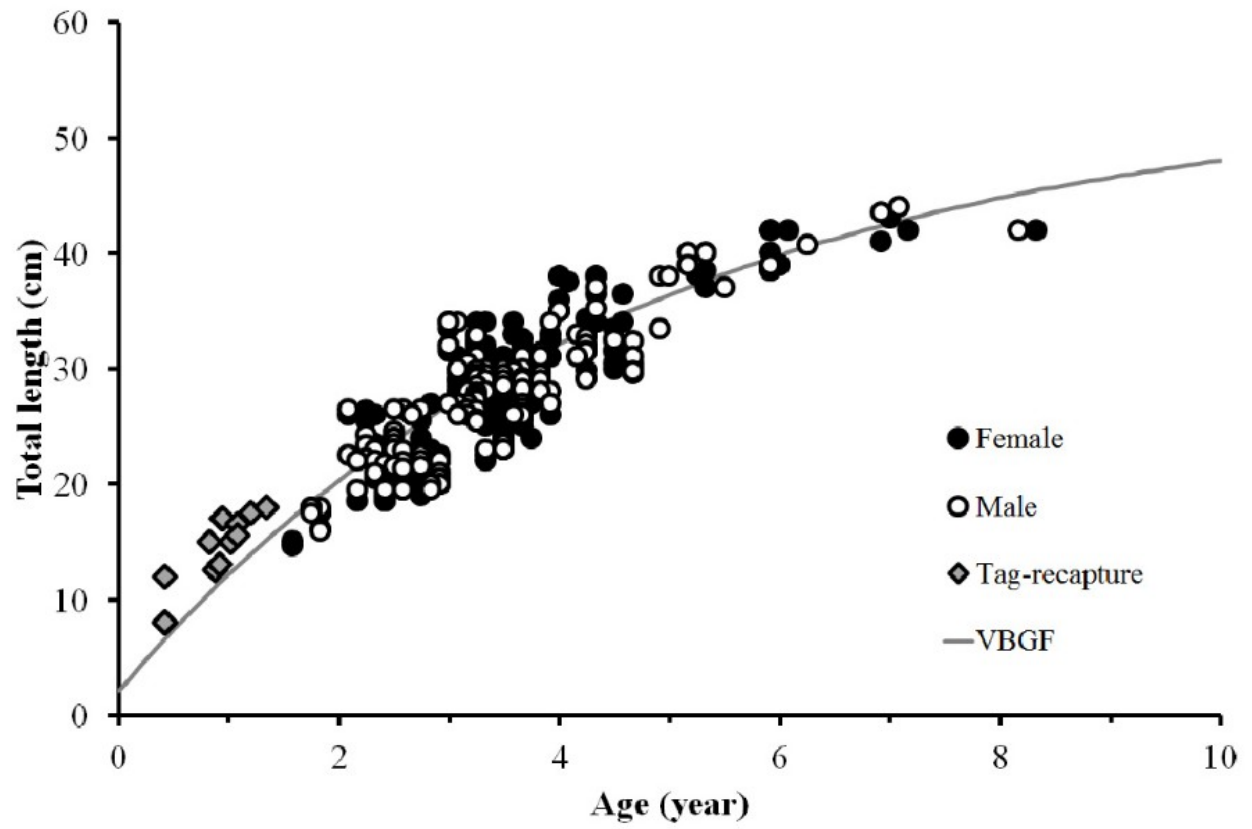


FIGURE 8. The von Bertalanffy growth curve for *R. sarba*. ●: tag and recapture data.

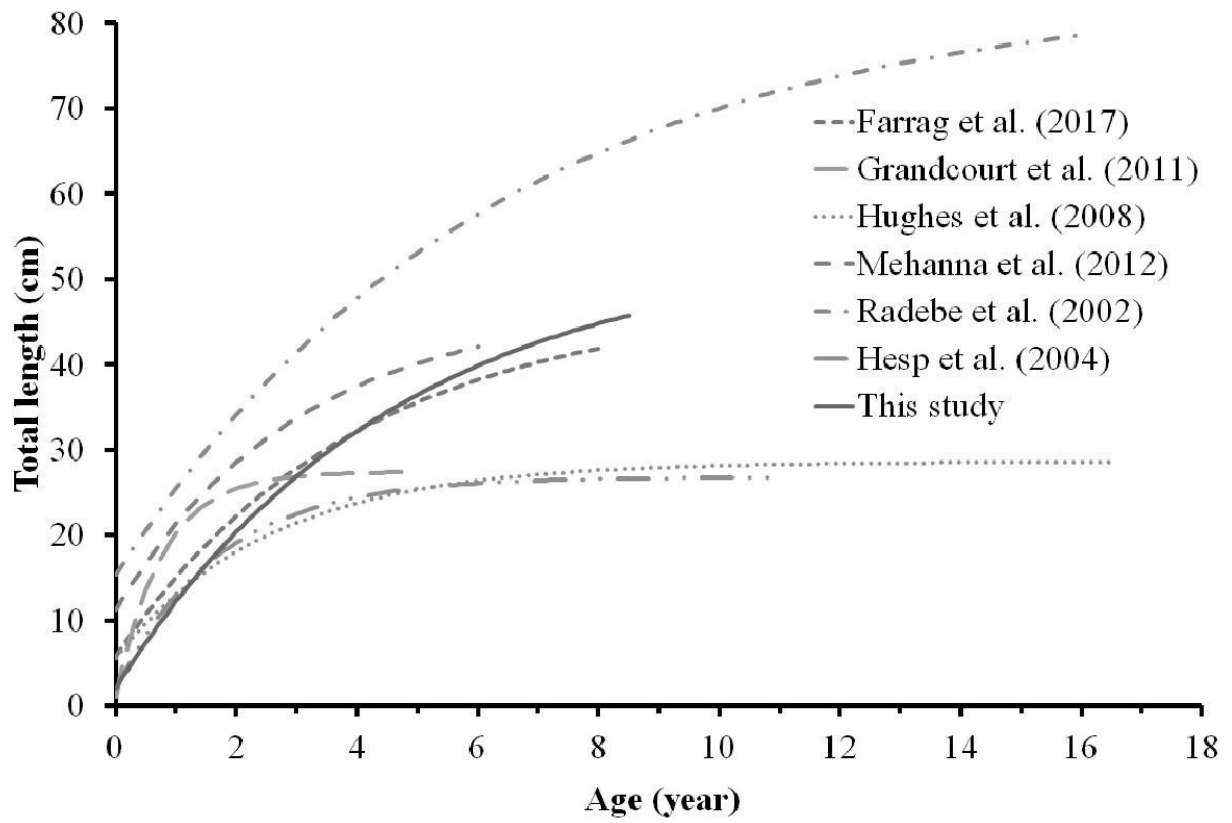


FIGURE 9. Comparison of the growth curves of *R. sarba* from different regions.